

WAVEGUIDE COUPLER KICK TO BEAM BUNCH AND CURRENT DEPENDENCY ON SRF CAVITIES*

G. Wu[#], Fermilab, Batavia, IL 60510, U.S.A.

H. Wang, C. E. Reece, R. A. Rimmer, Jefferson Lab, Newport News, VA 23606, U.S.A.

Abstract

JLAB SRF cavities employ waveguide type fundamental power couplers (FPC). The FPC design for the 7-cell upgrade cavities was optimized to minimize the dipole field kick. For continuous wave (CW) operation, the forwarding RF power will be at different magnitude to drive the different beam current and cavity gradient. This introduces some deviation from optimized FPC field for varying beam loading. This article analyzes the beam behavior both in centroid kick and head-tail kick under different beam loading conditions.

INTRODUCTION

For a waveguide coupler used on CEBAF SRF cavities, there is a transverse gradient of the electric field near beam axis. When the waveguide coupler was developed at Cornell University, the coupler field was measured through bead pull [1]. Such field was used to estimate the RF steering, i.e. beam kick in CEBAF linac [2, 3]. Stub was modified in waveguide coupler for 12-GeV upgrade cavities [4]. That resulted near zero coupler kick. Yet the optimization seemed relatively sensitive. During studies [5] of the coupler external Q and tolerance analysis, we found it was possible that the coupler kick could change due to the different beam load.

As shown in Figure 1, the field in the coupler near beam axis is a superposition of cavity decaying field, coupler forward wave and reflecting wave. When beam current changes, klystron power changes accordingly, the waveguide experiences a mixture of standing wave and traveling wave. While the standing wave has fixed zero magnetic field nodes, traveling wave component is not. Beam current can change the ratio of two wave components. Plus off-crest angle can cause superimposed field to have a moving zero node around beam axis in the coupler. This moving field can cause the originally optimized coupler kick to deviate.

NUMERICAL SIMULATION

To simulate the proper beam loading, we used HFSS code. As shown in Figure 2, the 7-cell cavity was replaced with two end cells to reduce the computational effort. Most of the electromagnetic codes do not handle the resistive cavity walls well. We instead inserted a coaxial antenna into the beam pipe to form a two port system. This way we can simulate the different beam load case with mixed wave around the coupler beam pipe region by adjusting the antenna length. To avoid the long

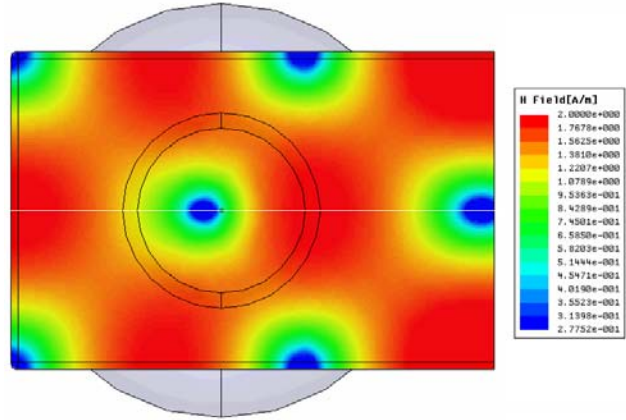


Figure 1: Magnetic field amplitude in coupler center plane.

computational time in scanning resonant frequency, we solved the model in eigen mode solution, then used the same mesh for harmonic scan near resonant frequency.

Once the fine scan (<10 Hz step) was completed, we went to find the resonant frequency and phase angle (ϕ_{crest}) to plot the field which truly represented the accelerating mode at the on-crest condition. The s-parameter S_{12} can be obtained at resonant frequency, so the condition of mixed wave can be matched to real beam loading of 7-cell cavity since only transmitted power through the beam pipe contributes to the beam. Post processing script was

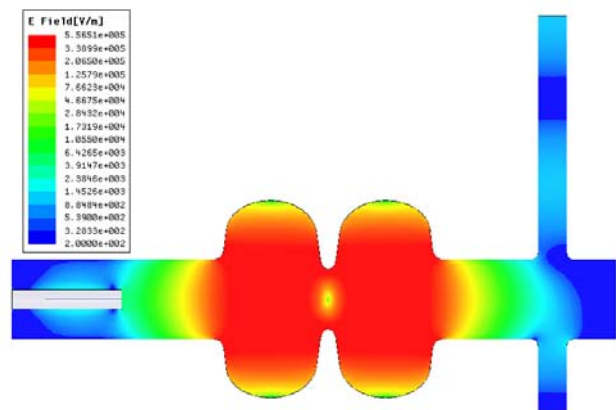


Figure 2: A two cell model with fundamental power coupler and beam pipe coaxial antenna. X-axis points from left to right; Z-axis points from bottom to top; origin sits at right end.

*Work supported by US DOE contract #DE-AC05-06OR23177

[#]genfa@fnal.gov

written to integrate the electromagnetic field on the beam axis around coupler.

KICKER FIELD

To simplify the computation, we assume the beam does not deviate off axis much. So the contributing kick field has two components of E_z and B_y . As an example, Figure 3 plots the change of magnetic field due to the change of the mixed wave on the coupler center axis.

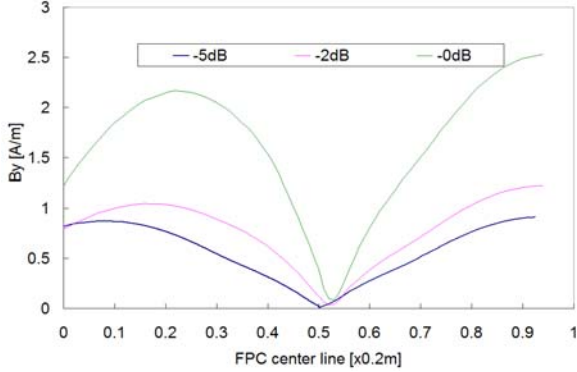


Figure 3: The coupler center magnetic field under different mixture of wave. 0.5 on x-axis represents the center of the coupler. 0 is at waveguide stub end.

In HFSS code, assuming beam travels on x -axis; field can be expressed in a form of

$$E_z(x) = E_z(x, \text{phase}) = E_z(x, \phi_{crest} + x \frac{f}{c} \cdot 2\pi)$$

$$B_y(x) = B_y(x, \phi_{crest} + x \frac{f}{c} \cdot 2\pi)$$

Using Lorentz force, we calculated the coupler kick by integrating a line section from x_1 to x_2 passing through coupler region:

$$\Delta P_z = -\frac{e}{c} \int_{x_1}^{x_2} [E_z(x, \phi_{crest} + (x-x_c) \frac{f}{c} 2\pi) + cB_y(x, \phi_{crest} + (x-x_c) \frac{f}{c} 2\pi)] dx$$

where x_c is the x coordinate of the right end cell equator plane in Figure 2.

Using the coordinate system in Figure 2, this is named downstream cavity to FPC kick. The upstream FPC to cavity kick can be expressed as:

$$\Delta P_z = \frac{e}{c} \int_{x_1}^{x_2} [E_z(x, \phi'_{crest} - (x-x_c) \frac{f}{c} 2\pi) + cB_y(x, \phi'_{crest} - (x-x_c) \frac{f}{c} 2\pi)] dx$$

ϕ'_{crest} equals ϕ_{crest} plus π . Then we can use the same HFSS solution file but two different post processing scripts with above two formulae.

For a limited length electron microbunch traveling on crest, centroid kick can be obtained using above two formulae. Change the ϕ_{crest} represents the head and tail of

the microbunch. Similarly, changing ϕ_{crest} can represent off-crest beam.

For CEBAF linac, the full beam current is 460 μ A. Using formula [6], we can estimate the klystron power P_g

$$P_g = \frac{V_c^2}{R_L} \frac{1+\beta}{4\beta} \left[\left(1 + \frac{I_0 R_L}{V_c} \cos\psi\right)^2 + \left(\tan\phi - \frac{I_0 R_L}{V_c} \sin\psi\right)^2 \right]$$

and the beam power P_b . $P_b = I_0^2 R_L$

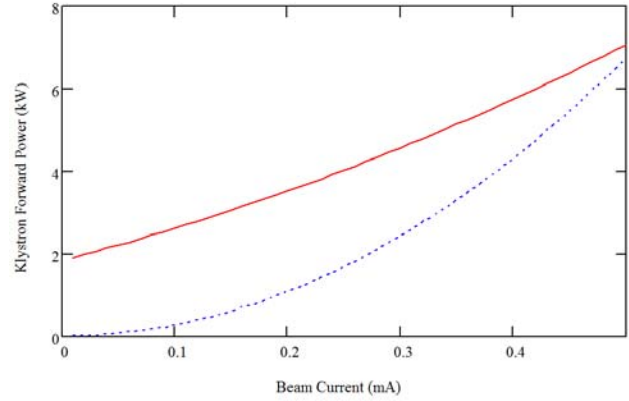


Figure 4: CEBAF 12GeV, LL cavity's klystron power (red) and beam power (blue) verse beam current at $E_{acc}=20$ MV/m.

To correlate the beam power to the HFSS simulation model, the ratio of power follows:

$$dB(I_0) = 10 \log \left(\frac{P_b(I_0)}{P_g(I_0)} \right)$$

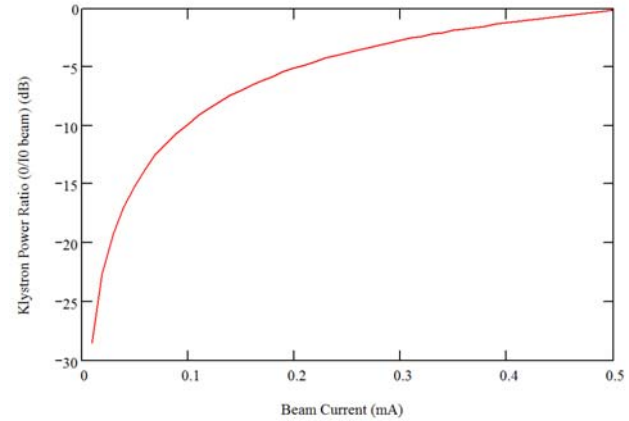


Figure 5: Correlation of beam current with dB number in HFSS model for the example of Figure 4.

For CEBAF 12GeV upgrade module, per coupler kick is listed in Table 1. The microbunch has small length as 1-degree in phase space. Head and tail of half degree off crest shows virtually same kick as centroid.

Table 1: Per coupler kick (centroid) for CEBAF 12-GeV upgrade cavity at $E_{acc}=20\text{MV/m}$.

Beam current [μA]	Klystron Power [W]	Kick: pc [MeV]	
		Cavity-FPC (downstream)	FPC-Cavity (upstream)
480	6,772	-7.04×10^{-4}	-3.10×10^{-4}
380	5,486	-4.13×10^{-4}	-1.81×10^{-4}
330	4,894	-2.79×10^{-4}	-1.81×10^{-4}
260	4,121	-1.97×10^{-4}	-0.78×10^{-4}
200	3,512	$+0.81 \times 10^{-4}$	$+0.41 \times 10^{-4}$

For the FEL-3 cryomodule in JLab FEL recirculation path and the SL21 cryomodule in CEBAF, the cavity is ‘‘OC’’ shape. The FPC coupler stub and the waveguide position to the cavity end cell are different from the 12GeV cavities. The centroid coupler kick is listed in Table 2. The microbunch was at 8-degree in phase space. The head and tail coupler kicks are listed in Table 3 and 4. It does show slight emittance degradation. The tail gets more kick at most off-crest degree.

Table 2: Per coupler kick (centroid) for FEL-3 cavity at -4° off-crest in 1st pass and $+10^\circ$ off-crest in 2nd pass with $E_{acc}=10\text{MV/m}$. For SL21 cavity, $<1\text{mA}$ beam current can be scaled for the kick.

Beam current [mA]	Klystron Power [W]	Kick: pc [MeV]	
		Cavity-FPC (downstream)	FPC-Cavity (upstream)
9.64	5166	-3.88×10^{-4}	-2.03×10^{-4}
7.03	3207	-2.36×10^{-4}	-1.42×10^{-4}
5.50	2327	-1.57×10^{-4}	-1.04×10^{-4}
4.51	1863	-1.28×10^{-4}	-0.55×10^{-4}
3.88	1611	-0.98×10^{-4}	-0.43×10^{-4}
3.16	1364	-0.69×10^{-4}	-0.35×10^{-4}
2.80	1257	$+0.51 \times 10^{-4}$	$+0.29 \times 10^{-4}$

Table 3: Per coupler kick (head) for FEL-3 cavity. Same conditions are as in Table 2.

Beam current [mA]	Klystron Power [W]	Kick: pc [MeV]	
		Cavity-FPC (downstream)	FPC-Cavity (upstream)
9.64	5166	-3.80×10^{-4}	-2.06×10^{-4}
7.03	3207	-2.32×10^{-4}	-1.46×10^{-4}
5.50	2327	-1.55×10^{-4}	-1.06×10^{-4}
4.51	1863	-1.26×10^{-4}	-0.56×10^{-4}
3.88	1611	-0.96×10^{-4}	-0.43×10^{-4}
3.16	1364	-0.68×10^{-4}	-0.35×10^{-4}
2.80	1257	$+0.50 \times 10^{-4}$	$+0.29 \times 10^{-4}$

Table 4: Per coupler kick (tail) for FEL-3 cavity. Same conditions are as in Table 2.

Beam current [mA]	Klystron Power [W]	Kick: pc [MeV]	
		Cavity-FPC (downstream)	FPC-Cavity (upstream)
9.64	5166	-3.88×10^{-4}	-2.03×10^{-4}
7.03	3207	-2.38×10^{-4}	-1.38×10^{-4}
5.50	2327	-1.58×10^{-4}	-1.01×10^{-4}
4.51	1863	-1.31×10^{-4}	-0.53×10^{-4}
3.88	1611	-1.00×10^{-4}	-0.42×10^{-4}

3.16	1364	-0.70×10^{-4}	-0.34×10^{-4}
2.80	1257	$+0.52 \times 10^{-4}$	$+0.28 \times 10^{-4}$

CONCLUSIONS

We calculated the coupler kick for both CEBAF upgrade cavity and FEL-3/SL-21 cavity. The kick shows only centroid kick is present and beam current dependent. The emittance growth based on head and tail estimation is negligible for short CEBAF microbunch. For FEL-3 cavity, the longer microbunch shows a bit emittance growth, yet quite manageable.

ACKNOWLEDGEMENT

We would like to thank the discussion we had with D. Douglas, J. Delayen, B. Yunn, R. Kazimi, and J. Preble all from Jefferson Lab.

REFERENCES

- [1] C. Reece, Cornell University Laboratory of Nuclear Studies SRF Note No. SRF860201EXA (February, 1986).
- [2] R.C. York, C. E. Reece, ‘‘RF steering in the CEBAF CW Superconducting Linac’’, Proc. of PAC 87, p1307, Washington DC (1987).
- [3] C. G. Yao, ‘‘Effects of Field Asymmetry in the Coupler,’’ Jefferson Laboratory Tech Note CEBAF-TN-89-183 (1989).
- [4] L. R. Doolittle, ‘‘Strategies for Waveguide Coupling for SRF Cavities’’, Proc. of LINAC 98, p246, Chicago (1998).
- [5] C. E. Reece, G. Wu, H. Wang, W. R. Hicks, E. F. Daly, J. Henry, and J. Preble, ‘‘Optimization of the SRF Cavity Design for the CEBAF 12 GeV Upgrade’’, this proceedings.
- [6] L. Merminga, J. Delayen, ‘‘On the Optimization of Qext under Heavy Beam Loading and in the Presence of Microphonics,’’ CEBAF Technote, TN 96-022, May 1996